This article has been accepted for publication in IEEE Journal of Radio Frequency Identification. This is the author's version which has not been fully edited and content may change prior to final publication. Citation information: DOI 10.1109/JRFID.2026.3662603

Analysis of UHF RFID Tag Antennas Using an Equivalent Circuit Approach

Pavel Nikitin, *Fellow, IEEE*, John Kim, *Member, IEEE* and KVS Rao, *Life Senior Member, IEEE*

***Abstract*— In this paper, we describe an equivalent circuit-approach to analyze one of the most common UHF RFID tag antennas, a T-matched dipole. We derive analytically closed-form expressions for all three tag resonant frequencies (two for tag sensitivity and one for backscatter). We show using a practical tag example, a 70 mm x 14 mm antenna designed for various items, how an equivalent circuit model can be effectively used for understanding its behavior and optimizing its performance. We also present experimental data that demonstrates good agreement with the model.**

***Index Terms*—Antennas, equivalent circuits, RFID tags**

I. Introduction

RFID TECHNOLOGY has a rich history [1]. Long range passive RFID operates primarily in far field and uses UHF frequencies. The current prevailing UHF standard, ISO 18000-6C (also known as EPC Gen2, or RAIN [2]), uses frequencies between 860 and 980 MHz. It now has many other uses beyond just reading the tags and allows one to do, for example, tag localization and sensing [3].

In passive UHF RFID systems, tag antenna gain and impedance match to the RFID IC (integrated circuit, or chip) over wide frequency band are critical. Improving tag performance while making tag antenna smaller is a challenging task because tag antenna dimensions limit maximum achievable antenna performance [4]. However, tag ICs with better sensitivity can help to reduce the size of the tag antennas while maintaining or improving tag performance.

The simplest tag antenna is an open circuited dipole [5]. Its use for RFID was analyzed in detail in previous works such as [6]. Its disadvantage is narrow impedance bandwidth due to the difficulty of wideband matching to complex IC impedance. To reduce the antenna size, dipole antennas used for tags can also be meandered, folded, or have capacitive loaded tips [7].

Today, majority of practical planar UHF RFID tags on the market use T-matched antennas. This matching method was known before [8] and is utilized in wireless applications, such as base station antennas [9]. T-matched RFID tag was first described in [10]. Over the past years, many other excellent works on T-matched tag antennas were published [11-21]. There also exist other variations of T-matched tag antennas. For example, the chip can be placed directly on the dipole, so called reversed T-matching [22]. Tags which are designed for metal objects also often employ T-matching [23-25].

Article submitted for review on October 17, 2025.
Pavel Nikitin, John Kim and KVS Rao are with Impinj, Inc., Seattle, WA 98109 (e-mail: nikitin@ieee.org)

Examples of T-matched tags are shown in Fig. 1. The most common antenna geometry (Fig. 1a) consists of a loop connected to a dipole, with chip placed on the loop (direct T-matching). The loop can also be electrically detached from dipole (Fig. 1b) but the coupling mechanism in both cases is the same, inductive coupling. Chip can also be placed directly on the dipole, resulting in reversed T-matching (Fig. 1c).

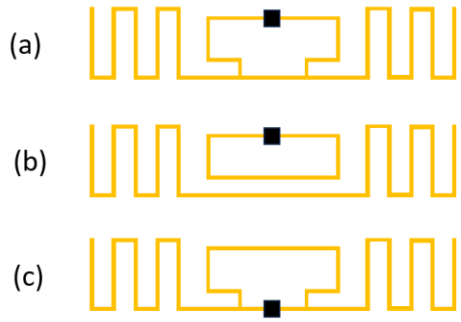

Fig. 1. Examples of T-matched RFID tags

T-matched tag antennas are very practical: they are cheap single layer structures that achieve a good broadband impedance match using only distributed traces and thus can be easily manufactured in large quantities. Thus, various meandered or folded T-matched tag antennas are often used in RFID applications that need cheap tags that work well on a variety of materials, such as tags designed for ARC specifications [26].

As it is well known, antenna impedance can be approximated by various broadband equivalent circuits [27-29]. Equivalent circuit models are a powerful tool and have been used, for example, in inductive HF RFID antenna modeling [30].

Many works on T-matched tag antennas [10-21] focused on tags optimized for specific applications. A number of those works [10, 11, 13-16, 18, 19, 21] as well as [24] described broadband equivalent circuits to represent the impedance of the T-matched tag antennas but did not relate it to the actual measurable tag characteristics (such as threshold sensitivity and backscatter) and tag resonances. Modeling of the tag precise backscatter using an equivalent circuit model was also not attempted. The resonant behavior of two inductively coupled LC-tanks was previously analyzed in some works on wireless power transfer systems [31, 32] but not specifically in context of UHF RFID systems and tags performance.

This article is a significant extension of our previous brief work [33]. We show in detail how the behavior of frequency-dependent threshold sensitivity and backscatter characteristics of T-matched tags can be fully understood as functions of antenna parameters through an analysis of an equivalent circuit model of a tag antenna. This model is a powerful tool that can be used to analyze and understand tag behavior as well as optimize its performance quickly, without time consuming EM simulations. This detailed analysis and its application to practical T-matched tag antenna design and optimization is the focus of this paper.

II. RFID Link Budget

In this section, we present RFID basic link budget equations, including specific definitions and formulas common in RFID (both in industry and academia). They are extensively used in this paper and provide a basis for our further analytical derivations.

The link budget of a monostatic RFID system is presented in Fig. 2. For simplicity, we assume that the reader antenna cable is lossless, there is no impedance mismatch between the reader antenna and the reader, and there is no polarization mismatch between reader and tag antennas. Reader transmitted signal with output power P_{tx} travels via cable and is radiated by a reader antenna with gain G_{reader} towards a tag located at a distance d away. The power incident on the tag, or POTF (Power on Tag Forward, term introduced by Voyantic [34] and now common in RFID industry), is defined by the propagation channel path gain G_{path} as

$$POTF = P_{tx}\, G_{reader}\, G_{path}\,. \tag{1}$$

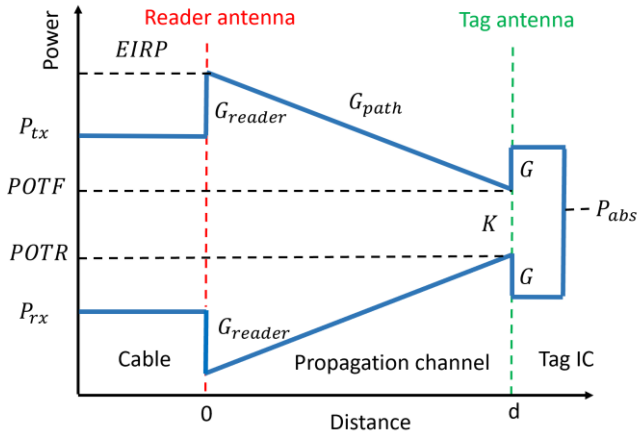

Fig. 2. Link budget of UHF RFID system

The graphical link budget in Fig. 2 uses log-linear power-distance loss, such as free space loss given by well-known Friis equation, $G_{path} = [\lambda/(4\pi d)]^2$. In general, propagation environment can include e.g. multipath [35, 36].

The power absorbed by the tag IC can be written as

$$P_{abs} = POTF \cdot G\,\tau\,, \tag{2}$$

where G is the tag antenna gain in the direction of reader antenna and τ is the tag impedance matching coefficient (also known as the power transmission coefficient) given by

$$\tau = 1 - |\rho_c|^2 = \frac{4R_cR_a}{|Z_c + Z_a|^2}. \tag{3}$$

For simplicity, we assume that tag and reader antennas are co-polarized (no polarization mismatch loss). In (3), $Z_c = R_c + jX_c$ is the complex chip impedance in absorbing state, $Z_a = R_a + jX_a$ is the complex antenna impedance, and ρ_c is the complex reflection coefficient between those complex impedances

$$\rho_c = \frac{Z_c - Z_a^*}{Z_c + Z_a}. \tag{4}$$

RFID IC impedance in absorbing state at any frequency can be well approximated by a parallel combination of resistance R_p and capacitance C_p as $Z_c = R_c + jX_c = R_p||1/(j\omega C_p)$. Note that resistance R_p and capacitance C_p are dependent on power as well as communications mode. If their values at threshold are known (for example, from IC datasheet), then the IC turn-on threshold can be defined either in terms of threshold absorbed power P_{th} or in terms of threshold voltage V_{th} on IC which are related as

$$P_{th} = \frac{|V_{th}|^2}{2\,R_p} = \frac{|V_{th}|^2}{2\,|Z_c|^2} R_c \tag{5}$$

Passive tag can be viewed as an active source of modulated RF power, producing backscattered modulated power, or POTR (Power on Tag Reverse, also a term introduced by Voyantic and now common in RFID industry).

When tag backscatters, the modulator (usually, a transistor in parallel with antenna) turns on and off. This effect can be approximately modeled as modulation resistor R_{mod} being applied in parallel with the antenna. Thus the equivalent circuit of a generic RFID tag (neglecting for simplicity the contact resistances or parasitic and strap capacitances) can be drawn as shown in Fig. 3. Thevenin open-circuit voltage V_o induced on antenna terminals by incident RF signal from the reader can be calculated as

$$|V_o|^2 = 8\,POTF \cdot G \cdot R_a \tag{6}$$

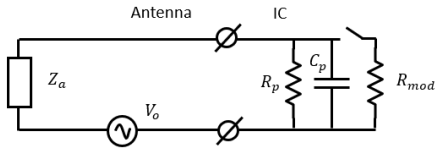

Fig. 3. Equivalent Thevenin circuit of RFID tag.

The differential modulated power backscattered by the tag can be calculated as re-radiated power due to the vector difference between the currents running through the tag antenna when chip switches between absorbing and modulating states. That power is related to incident POTF via backscatter factor K as

$$POTR = POTF \cdot K\,, \tag{7}$$

where backscatter factor K is related to differential RCS (radar cross-section) σ_d described in [37, 38] and differential reflection coefficient $\Delta\Gamma = |\rho_c - \rho_m|^2$ as

$$K = \frac{4\pi\sigma_d}{\lambda^2} = \frac{1}{2}G^2|\Delta\Gamma|^2\,. \tag{8}$$

This article has been accepted for publication in IEEE Journal of Radio Frequency Identification. This is the author's version which has not been fully edited and content may change prior to final publication. Citation information: DOI 10.1109/JRFID.2026.3662603

For simplicity, we will assume that chip impedance in absorbing state Z_c is the same during forward (reader-to-tag) and reverse (tag-to-reader) communication. This is not always the case because tag IC power consumption is different in those communication periods. In (8), the coefficient ½ arises from assumed 50% duty cycle of tag modulation (think of a tag as an active RF transmitter that is on half of the time while it backscatters). That equation also assumes that that power of all spectral components of backscattered signal harmonics is summed (in other words, power of tag signal includes carrier component too) – this is how POTR is defined and measured by Voyantic Tagformance receiver. If, for example, only sidebands of received differential tag signal are taken into account, the coefficient K in (9) becomes K=¼ (see [38]).

In $\Delta\Gamma$, ρ_c is given by (4) and ρ_m is the complex reflection coefficient between the antenna impedance and chip impedance in modulating state (which is $Z_c \parallel R_{mod}$) given by

$$\rho_m = \frac{Z_c \parallel R_{mod} - Z_a^*}{Z_c \parallel R_{mod} + Z_a} . \quad (9)$$

That backscattered modulated signal travels back to the reader through the same propagation channel with the same path gain G_{path}. The power received by the reader (also known in wireless as Received Signal Strength Indicator, or RSSI) is

$$P_{rx} = POTR \cdot G_{path}\, G_{rda} . \quad (10)$$

The quantities of main interest to tag antenna designers are POTF and POTR at tag activation threshold. From (2), threshold tag sensitivity $POTF_{th}$ (needed for IC to turn on) is related to IC threshold sensitivity P_{th} as

$$POTF_{th} = \frac{P_{th}}{G \cdot \tau} . \quad (11)$$

Using (7), (8) and (11), we can obtain that

$$POTR_{th} = \frac{1}{2} P_{th}\, G\, \frac{|\Delta\Gamma|^2}{\tau} . \quad (12)$$

Equations (11) and (12) give threshold POTF and POTR at threshold of tag activation.

In reality, IC impedance Z_c is strongly power dependent. Hence, if the tag is moved closer to the reader, it becomes overdriven above that threshold. However, note that (11) and (12) remain valid for any power level (just use P_{abs} instead of P_{th}). Thus, in order to calculate, for example, how much power is actually absorbed and backscattered by the tag placed at a certain distance (at the incoming power level POTF), one would need to solve the following transcendental equation

$$P_{abs} = POTF \cdot G\, \tau\,(P_{abs}) . \quad (13)$$

Solution to this equation requires knowledge of how chip impedance in both absorbing and modulating states (ultimately defined by R_p, C_p, and R_{mod}) changes as a function of absorbed power P_{abs}. Once P_{abs} is found from (13), POTR is then calculated from (12) using $|\Delta\Gamma|^2$ and τ that are calculated at that absorbed power level. Then one can easily calculate, for example, POTR vs POTF behavior which is important to find ARC backscatter margins.

One question that sometimes arises is: can POTR be greater than POTF? The answer is yes: as one can see from (8), POTR can reach $2G^2$, because factor $|\Delta\Gamma|^2$ is bounded by Smith chart (its maximum possible value is 4). So, for tag antenna with higher gain values, POTR can exceed POTF. Note that the power is still conserved: conducted modulated power from tag IC into tag antenna can never exceed conducted power available to tag IC from tag antenna.

Another useful equation that follows directly from previously derived equations is

$$P_{tx} P_{rx} = POTF \cdot POTR . \quad (14)$$

This equation relates RF conducted powers in reader transmitter and receiver to directly measurable tag characteristics (POTF and POTR). This equation is independent of path loss (it remains valid for any propagation environment – free space, multipath, etc.), valid at any power level (threshold and above), and is also completely independent of the gain of the reader antenna. It allows one to easily calculate, for example, a received conducted power at the reader if the reader P_{tx} and tag POTF and POTR are known.

III. T-MATCHED TAG ANTENNA ANALYSIS

RFID tag antennas must have inductive reactance for matching to the capacitive chip impedance. In general, impedance of such antennas can be represented in a narrow band around the dipole resonance by simple equivalent circuits [27-29]. However, wideband equivalent circuit requires a different circuit topology which depends on antenna geometry and frequency band of approximation. Below, we analyze most common RFID antenna geometry, a T-matched dipole, which includes all geometries shown in Fig. 1.

A. T-matched tag properties

Typical impedance, threshold POTF and threshold POTR of a T-matched tag are shown in Fig. 4. Note that POTF has two minima, at frequencies ω_a and ω_b while POTR has one maximum at the frequency ω_c.

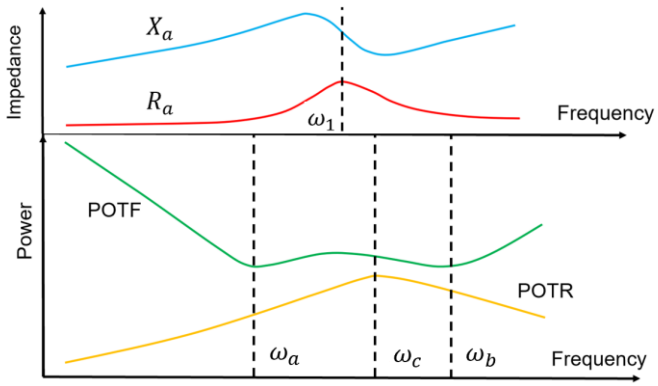

Fig. 4. Antenna impedance, POTF and POTR of a T-matched tag.

Threshold POTF and POTR behavior shown in Figure 4 is well known to many RFID tag antenna designers. Tag resonant frequencies ω_a, ω_b, and ω_c are very important for the design of tags that must work well on a variety of materials.

B. Equivalent Circuit

Threshold POTF and POTR behavior shown in Fig. 4 can be fully explained using equivalent circuits for T-matched tag antenna shown in Fig. 5. Those circuits appeared in literature before in various forms [10, 11, 13-16, 18, 19, 21, 24].

Note that while any antenna can be represented using simpler circuit models (e.g., RL, RC, or RLC), those models would be narrowband (values of circuit components would be frequency dependent). Advantages of circuit model shown in Fig. 5 are that it is broadband, using fixed circuit element values.

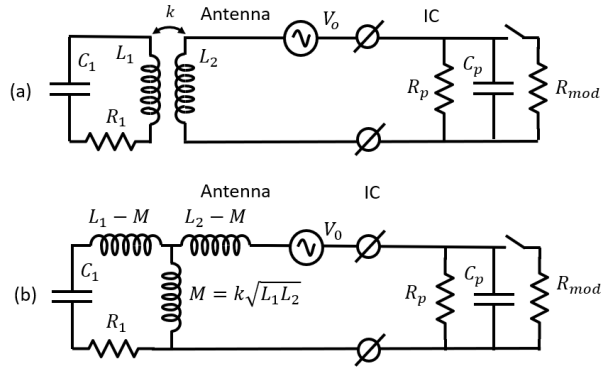

Fig. 5. Two equivalent broadband circuits of a T-matched antenna: transformer-based (a) and with T-network of inductors (b).

Top circuit in Fig. 5 is a transformer-based circuit that consists of a series RLC-circuit (representing the impedance of a dipole antenna around its fundamental resonance), inductively coupled to a parallel RLC circuit (that represents a loop loaded with a capacitive chip). This circuit appeared in various forms in [10, 11, 13, 15, 19]. The same circuit can be redrawn without using a transformer, but rather by using a T-network of inductors as shown in bottom circuit in Fig. 5. This circuit form was used in [14, 16, 18, 21]. The same equivalent circuit can also be represented using π-network [39], but that representation is far less commonly used in RFID literature, so we omit its analysis in this paper.

The two circuits in Fig. 5 are equivalent and have three key defining parameters. First parameter is a natural resonant frequency of a dipole, $\omega_1 = 1/\sqrt{L_1 C_1}$. Second parameter is a natural resonant frequency of a loop loaded with chip, $\omega_2 = 1/\sqrt{L_2 C_p}$. The third parameter is a coupling coefficient k between loop and dipole.

The impedance of a tag antenna as seen by RFID chip can be found, using e.g. transformer version of equivalent circuit (top circuit in Fig. 5), from the loop impedance $Z_{loop} = j\omega L_2$ and dipole impedance $Z_{dipole} = R_1 + j\omega L_1 + 1/(j\omega C_1)$ as

$$Z_a = Z_{loop} + \frac{\omega^2 M^2}{Z_{dipole}} = j\omega L_2 + \frac{\omega^2 M^2}{R_1 + j\omega L_1 + 1/(j\omega C_1)}. \quad (15)$$

At dipole resonant frequency ($\omega = \omega_1$), the reactance is entirely defined by loop inductance L_2 while the resistance is entirely defined by mutual inductance M and the dipole resistance R_1 (which includes both radiation resistance and losses). From (15), one can easily derive general expressions for T-matched antenna series resistance and reactance as

$$R_a = \frac{\omega^2 M^2 R_1}{R_1^2 + \omega^2 L_1^2 \left(1 - \frac{\omega_1^2}{\omega^2}\right)^2}, \quad (16)$$

$$X_a = \omega \left[L_2 - M \frac{\omega^2 L_1^2 \left(1 - \frac{\omega_1^2}{\omega^2}\right)\left(2 - \frac{\omega_1^2}{\omega^2} - \frac{M}{L_1}\right)}{R_1^2 + \omega^2 L_1^2 \left(1 - \frac{\omega_1^2}{\omega^2}\right)^2} \right]. \quad (17)$$

Antenna impedance can also be rewritten in terms of parallel antenna resistance R_{pa} and parallel antenna reactance:

$$Z_a = R_a + jX_a = R_{pa} || jX_{pa}, \; X_{pa} = R_{pa} \frac{R_a}{X_a}. \quad (18)$$

We can derive an elegant expression for R_{pa}:

$$R_{pa} = \frac{L_2}{k^2 L_1 R_1} \left[R_1^2 + \omega^2 L_1^2 \left(1 - k^2 - \frac{\omega_1^2}{\omega^2}\right)^2 \right], \quad (19)$$

We will use this expression later in this paper.

C. Frequencies of POTF minima

To find POTF resonances (frequencies of POTF minima), assume that antenna gain G is a slowly changing function of frequency compared to impedance matching coefficient τ, which is true for many RFID tags. Then, the minima of $POTF_{th}$ are defined solely by the resonant frequencies of the tag equivalent circuit.

To simplify the problem, let us also assume that $R_p \to \infty$ and $R_1 \to 0$. This assumption (eliminating lossy resistive components from the circuit) does not change the resonant frequencies of the circuit transfer function and can be viewed as a specific case of the two extra element theorem [40].

The circuit shown in Fig. 5 (top circuit) then turns into a simple circuit shown in Fig. 6, with two inductively coupled lossless LC tanks.

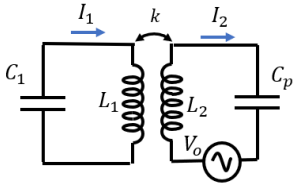

Fig. 6. Simplified equivalent circuit from Fig. 5(a)

Currents I_1 and I_2 in this circuit can be found as

$$\begin{pmatrix} I_1 \\ I_2 \end{pmatrix} = \hat{Z}^{-1} \begin{pmatrix} 0 \\ Vo \end{pmatrix}. \quad (20)$$

The impedance matrix $\hat{Z}$ of this circuit is:

$$\hat{Z} = \begin{bmatrix} \frac{1}{j\omega C_1}(1 - \omega^2 L_1 C_1) & -j\omega M \\ -j\omega M & \frac{1}{j\omega C_p}(1 - \omega^2 L_2 C_p) \end{bmatrix}. \quad (21)$$

The transfer function of this circuit reaches maxima at resonances which occur when the determinant of the impedance matrix $\hat{Z}$ is zero (current in either LC tank becomes infinite). This gives a quadratic equation for ω^2 expressed as

$$\frac{k^2 \omega^4}{\omega_1^2 \omega_2^2} = \left(1 - \frac{\omega^2}{\omega_1^2}\right)\left(1 - \frac{\omega^2}{\omega_2^2}\right). \quad (22)$$

Solutions to that quadratic equation are the two frequencies of POTF minima, $\omega_a = 2\pi f_a$ and $\omega_b = 2\pi f_b$, given by

This article has been accepted for publication in IEEE Journal of Radio Frequency Identification. This is the author's version which has not been fully edited and content may change prior to final publication. Citation information: DOI 10.1109/JRFID.2026.3662603

$$\omega_{a,b}^2 = \omega_1^2 \frac{1+\xi^2 \pm \sqrt{(1-\xi^2)^2+4k^2\xi^2}}{2(1-k^2)}, \quad (23)$$

where

$$\xi = \omega_2/\omega_1 \quad (24)$$

is the ratio of the loop natural resonant frequency ω_2 to the dipole natural resonant frequency ω_1.

D. Frequency of POTR maximum

To find the location of POTR maximum, we will use the same assumption for tag antenna gain G (that tag antenna gain is a slowly changing function of frequency). Let us also assume that the modulating resistance $R_{mod} \to 0$. This assumption is true for majority of tag chips where $R_{mod} \ll R_p$. Then we can simplify factor in (12) as

$$\frac{|\Delta\Gamma|^2}{\tau} = \frac{|Z_m - Z_c|^2}{|Z_m + Z_a|^2} \frac{R_a}{R_c} \approx \frac{R_p}{R_{pa}}. \quad (25)$$

Because R_p is frequency independent, POTR maximum will occur when R_{pa} reaches minimum. We can easily see from (19) that it happens at the frequency $\omega_c = 2\pi f_c$

$$\omega_c^2 = \frac{\omega_1^2}{1-k^2}. \quad (26)$$

This is the frequency of POTR maximum (POTR peak). Note that it is higher than the frequency ω_1 of dipole resonance.

E. Values of POTR at maximum and POTF at minima

To find the value of POTR maximum, we can use equations (12) and (25). The maximum threshold POTR value at the POTR resonance ($\omega = \omega_c$) is then given by

$$\max(POTR_{th}) = \frac{1}{2} P_{th}\, G \frac{R_p}{R_1} k^2 \frac{L_1}{L_2} \quad (27)$$

Value of threshold POTF at resonances ω_a and ω_b can also be found in a similar way from (11) and (23) but the expressions are far more complicated and less intuitive, so we omit those.

F. Significance and discussion of derived formulas

Analytical formulas derived above allow an engineer to qualitatively better understand the behavior of tag resonances without running multiple EM simulations or trying multiple equivalent circuit values.

One can see, for example, from (23) that POTF minima frequencies ω_a and ω_b depend on dipole natural resonance ω_1, coupling coefficient k, and natural loop frequency ω_2 (defined by chip capacitance and loop inductance).

Equations (12) and (25) show that threshold POTR curve is independent of the chip capacitance. That means that any additional capacitance (due to parasitic or to capacitors in self-tunings ICs) does not affect threshold POTR curve.

Equation (26) reveals that POTR maximum frequency ω_c is a function of only dipole natural resonance frequency ω_1 and coupling coefficient k. That frequency ω_c does not depend on neither chip nor loop parameters.

Equation (27) gives another useful insight to tag designers: it tells that the backscatter is stronger for tags which have higher k and L_1, while having lower R_1 and L_2 values.

Equations (23) and (26) have another practical significance: because resonances ω_a, ω_b, ω_c are easily measurable (from measured threshold POTF and POTR curves), they can be used to directly find ω_1, ω_2, k from measured threshold tag responses. This allows one, for example, to determine dielectric or magnetic properties of the tagged material [41, 42] or to extract tag antenna equivalent circuit just from threshold POTF and POTR curves (by reducing the number of variables needed for curve-fitting using min-squares optimization).

G. Behavior of tag resonant frequencies

Plot in Fig. 7 shows the dependence of frequencies ω_a, ω_b, ω_c given by (23) and (26) on coupling factor k for two cases (all frequencies are normalized to ω_1).

In one case, ξ =0.8 (loop natural frequency is smaller than dipole natural frequency, or $\omega_2 \leq \omega_1$). This is very common case in tag antenna designs with small footprint, which often use dipoles that resonate at higher frequencies. In another case, ξ =1.2 (loop natural frequency is higher than dipole natural frequency, or $\omega_2 \geq \omega_1$).

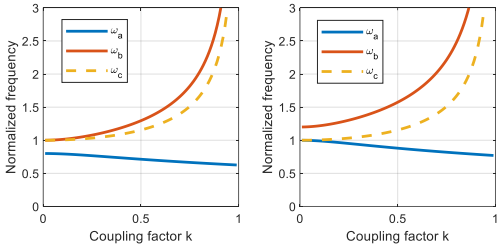

Fig. 7. POTF and POTR resonant frequencies ω_a, ω_b, ω_c as functions of coupling factor k for ξ =0.8 (left plot) and ξ =1.2 (right plot)

We can see that in the case of weak coupling ($k \to 0$), POTR resonance ω_c is always at the dipole natural resonance ω_1. As coupling increases, POTF resonances separate, and POTR resonance (ω_c) follows the higher POTF resonance (ω_b) but stays bound by the two POTF resonances (ω_a, ω_b).

Indeed, one can show mathematically from (23) and (26) that, for any ξ, POTR resonant peak frequency is always contained between the two POTF resonant minima frequencies:

$$\omega_a \leq \omega_c \leq \omega_b. \quad (28)$$

Fig. 8 shows the dependence of frequencies $\omega_a, \omega_b, \omega_c$ given by (23) and (26) on ξ, for two cases (again, all frequencies are normalized to ω_1). One case is lightly coupled tag (k =0.05), another case is heavily coupled tag (k =0.25).

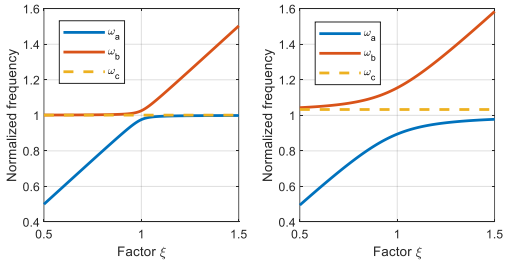

Fig. 8. POTF and POTR resonant frequencies as functions of ξ for k =0.05 (left plot) and k =0.25 (right plot).

This article has been accepted for publication in IEEE Journal of Radio Frequency Identification. This is the author's version which has not been fully edited and content may change prior to final publication. Citation information: DOI 10.1109/JRFID.2026.3662603

We can see in both cases that when ξ is low (that means loop resonant frequency is lower than dipole resonant frequency), changing ξ (e.g. by changing the loop length) mostly affects the lower POTF resonance (ω_a). For higher values of ξ, changes in ξ mostly affect the upper POTF resonance (ω_b). Figure 8 clearly illustrates that behavior.

Tag resonances behavior described above is empirically known to many experienced RFID tag antenna designers. Analytical equations presented in this paper now provide an additional useful mathematical insight into it.

IV. Practical Example

A. Tag antenna design

As an example, consider a practical RFID tag antenna shown in Fig. 9: a 70 mm x 14 mm tag antenna with M700 series IC [43]. This is a compact tag with a footprint < 1,000 mm^2 that was designed by our antenna group for a wide variety of retail applications and ARC specs using a process similar to the one described in [44]. It is available as a product through various manufacturers [45]. We use this antenna as an example to demonstrate the capabilities of equivalent circuit approach.

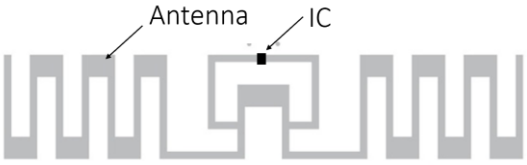

Fig. 9. E702 RFID tag (70 mm x 14 mm).

Key design parameters for this T-matched antenna with meandered dipole included the dipole resonant frequency, the loop inductance, and the coupling between the loop and the dipole. Antenna was simulated in CST EM simulator [46], using multi-layer Method of Moments solver, with gain monitored in normal direction (perpendicular to the plane of the antenna). Threshold POTF and POTR were calculated using equations (11) and (12) until desired ARC specs were met. The final inlay design was adjusted to make sure tag performs as desired and meets desired ARC specs when converted into wet inlay format and applied to tested items.

B. Measurements and simulations

The tag was manufactured using etched aluminum layer on 0.05 mm polyethylene therephtalate (PET) substrate and direct-die attachment of RFID IC. The tag (dry inlay) is shown in Fig. 10. Our tag measurement setup is shown in Fig. 11.

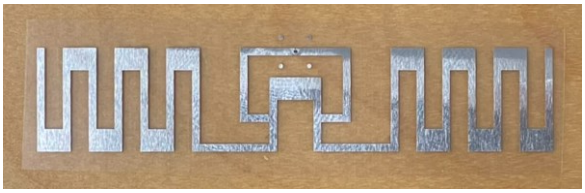

Fig. 10. Manufactured E702 tag.

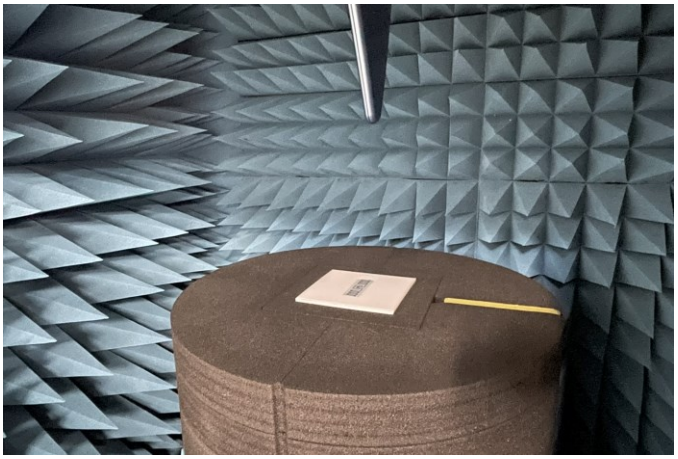

Fig. 11. Anechoic chamber test setup for tag measurement.

Test equipment (Voyantic Tagformance Pro) is connected to a top mounted broadband log-periodic antenna. Tag is placed flat on the RF transparent foam stand inside an anechoic chamber, facing the antenna. In Fig. 11, the tag is attached to dielectric.

In tag simulations, measurements, and analysis throughout this paper, we used the following two cases: air and dielectric (polyoxymethylene plastic, eps=2.96, tan=0.045, plate size 130 mm x 130 mm x 3.125 mm).

Measured and simulated threshold POTF and POTR, calculated using (11) and (12), using EM simulated gain and impedance are shown in Fig. 12. The following IC parameters were used for modeling the tag: R_p =2.4 KOhm, C_p =1 pF, P_{th} =-21 dBm, R_{mod} = 25 Ohm. The autotune feature of M730 IC was disabled to make POTF resonances more visible. Measured and modeled threshold POTF and POTR curves are in good agreement, both in air and on dielectric.

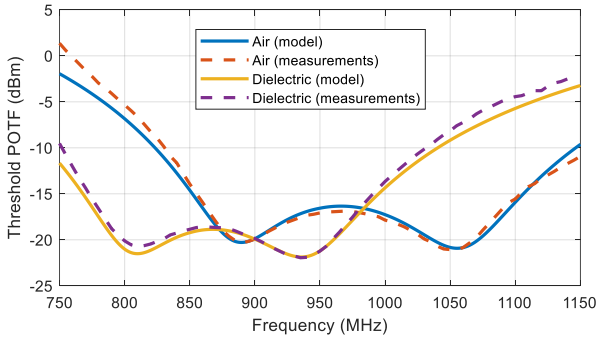

Fig. 12. Threshold POTF of E702 tag.

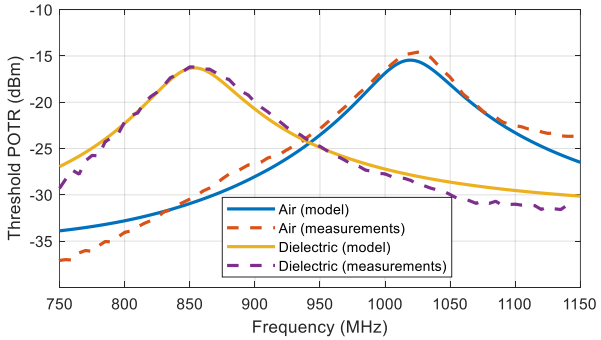

Fig. 13. Threshold POTR of E702 tag.

C. *Equivalent circuit extraction*

Equivalent circuit of any antenna can be extracted by approximating the impedance of this antenna (obtained from EM simulation or measurement) in the frequency band of interest using specific circuit topology. In our case, circuit topology is given by Fig. 5, antenna impedance is obtained from EM simulations, and the frequency band of our interest includes both POTF and POTR resonances.

To find circuit element values, one can use standard method with blind min-square optimization [47] but it would require 5-dimensional space search (circuit has five unknown elements: R_1, L_1, C_1, k, L_2). We present here another, more elegant approach which requires only a two-dimensional space search.

At resonant frequency ω_1, antenna resistance and reactance can be written using (16) and (17) as

$$R_a(\omega_1) = \frac{\omega_1^2 k^2 L_1 L_2}{R_1}, \qquad X_a(\omega_1) = \omega_1 L_2, \tag{29}$$

Also, we know that $\omega_1 = 1/\sqrt{L_1 C_1}$. That gives us three equations for our five unknowns. Now we can proceed with standard min-square error optimization over just two variables.

Let us choose, for example, R_1 and L_1 as unknown variables. After discretizing search space and setting search limits, we can start optimization. For each possible combination of R_1 and L_1 within our search space, we can calculate C_1, k, and L_2 as:

$$L_2 = \frac{X_a(\omega_1)}{\omega_1}, \; C_1 = \frac{1}{\omega_1^2 L_1}, \; k = \frac{1}{\omega_1}\sqrt{\frac{R_a(\omega_1) R_1}{L_1 L_2}}. \tag{30}$$

Then we calculate min. squares error based on simulated antenna impedance Z_a and impedance Z_{ckt} produced by the equivalent circuit at discrete frequencies $\omega_1 \ldots \omega_N$:

$$MSE = \frac{1}{N}\sum_{i=1}^{N} |Z_a(\omega_i) - Z_{ckt}(\omega_i)|^2 \tag{31}$$

Minimizing the cost function given by (31) allows one to find equivalent circuit element values R_1 and L_1.

The values of equivalent circuit elements extracted to approximate antenna impedance in 750-1150 MHz band and resonant frequencies are summarized in Table I, which also gives natural resonant frequencies of loop and dipole. Not that both in air and on dielectric dipole inductance L_1, loop inductance L_2, and coupling coefficient k all remains approximately the same, while dipole resistance and capacitance change significantly.

TABLE I. EQUIVALENT CIRCUIT VALUES AND NATURAL RESONANCES FOR E702 TAG

Element	Description	Air	Dielectric
R_1	Dipole resistance	91 Ohm	71 Ohm
L_1	Dipole inductance	271 nH	281 nH
C_1	Dipole capacitance	92 pF	127 pF
k	Coupling coefficient	0.16	0.14
L_2	Loop inductance	30 nH	31 nH
ω_1	Dipole resonance	1008 MHz	842.5 MHz
ω_2	Loop resonance	918.9 MHz	903.9 MHz

The equivalent circuit extracted using procedure above approximates the simulated antenna impedance very well as shown in Fig. 14.

The equivalent circuit extraction method described above is based on using the knowledge of tag antenna impedance, obtained from EM simulations. However, even with that knowledge, we also need to know the gain of tag antenna to calculate POTF and POTR. Gain of E702 tag, on air and dielectric, obtained from EM simulations is shown in Fig.15.

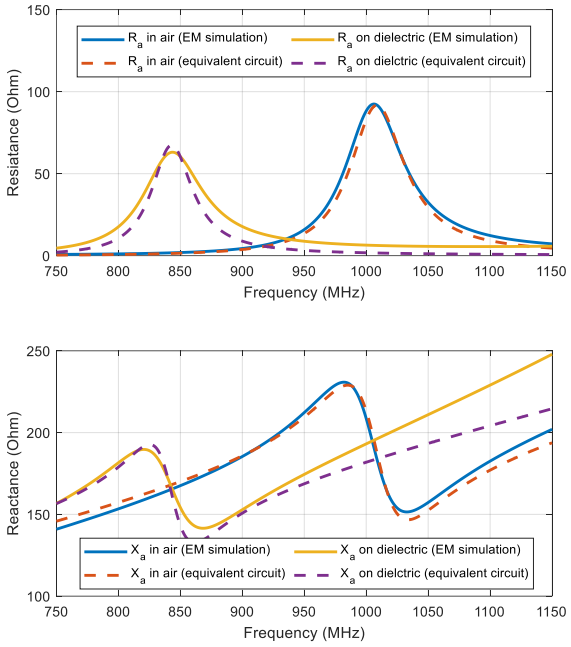

Fig. 14. Antenna impedance and its approximation by equivalent circuit.

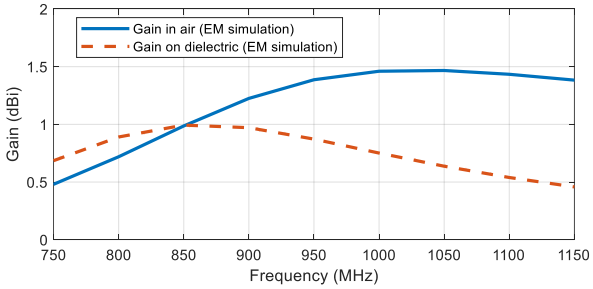

Fig. 15. Simulated antenna gain (IEEE) in normal direction (orthogonal to antenna plane) in air and on dielectric.

Note that extraction of tag antenna equivalent circuit can also be done from tag measurements. For example, combining equations (11) and (12) allows us to write:

$$POTF_{th}\, POTR_{th} = \frac{1}{2} P_{th}^2 \frac{|\Delta\Gamma|^2}{\tau^2}. \tag{32}$$

If tag IC sensitivity P_{th} is known, one could extract tag equivalent circuit model parameters by searching through possible space of values while trying to find the best fit, using circuit model in Fig. 3, to the product of threshold tag sensitivity and backscatter (which can easily be measured using standard RFID testing equipment, such as Voyantic [34]). Note that knowledge of tag antenna gain is not needed for that process because tag gains doesn't participate in equation (32).

This article has been accepted for publication in IEEE Journal of Radio Frequency Identification. This is the author's version which has not been fully edited and content may change prior to final publication. Citation information: DOI 10.1109/JRFID.2026.3662603

D. *Antenna analysis and optimization*

An equivalent circuit model of a tag antenna can be used to analyze and optimize an existing tag without running multiple EM simulations. A designer can change equivalent circuit parameters that affect loop, dipole, coupling, and then instantaneously see what effect on tag performance those changes would have. That iterative process can be repeated until desired tag performance is obtained. At that exploration stage, antenna gain from initial EM simulations can be used. If satisfied, now armed with the knowledge of what needs to be changed (e.g., dipole, loop, coupling), designer can go back to EM simulator and implement those changes by modifying antenna geometry (e.g., reduce loop inductance, make dipole longer, make coupling less).

Of course, in realistic compact RFID tags, there exists an interaction between all antenna geometry elements (dipole sections, dipole meanders, loop). An equivalent circuit cannot predict how the gain of an antenna would be affected by equivalent circuit changes. The final stage of tag optimization would still require EM simulations.

As an example, let us say we want to optimize this tag design for a particular application and need to understand the effect of adjusting the loop. Such knowledge helps, for example, to adapt this antenna to other chips which may have other chip capacitance. To do this, let us investigate the influence of the loop inductance L_2 on threshold POTF and POTR of our tag.

We can easily do by changing L_2 value in circuit values given in Table I, then recomputing antenna impedance using (16) and (17), and finally recalculating threshold POTF and POTR using equations (11) and (12) and gain given in Fig. 15.

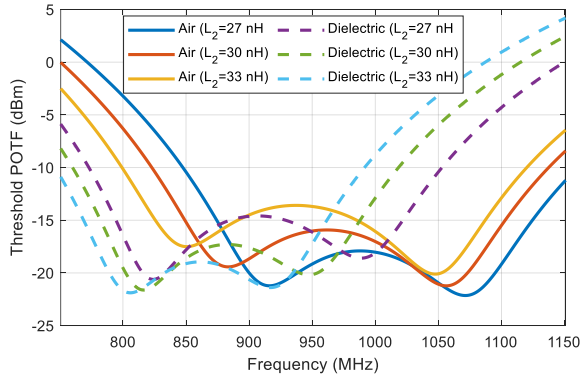

Fig. 16. Effect of loop inductance on tag POTF.

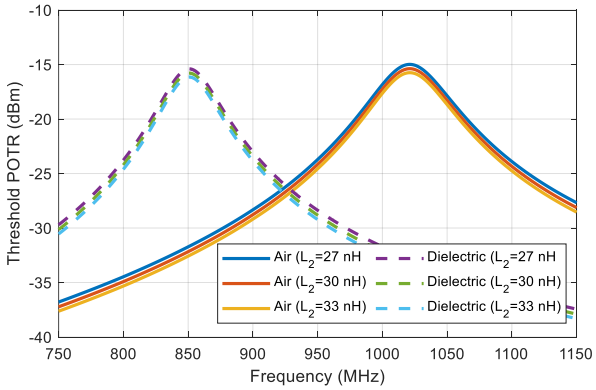

Fig. 17. Effect of loop inductance on tag POTR.

Results of this exercise are given in Fig. 16 and 17. As one can expect, both in air and on dielectric POTF resonant frequencies change as the loop inductance changes but POTR resonant frequency remains constant. The backscatter (threshold POTR) is stronger for lower values of L_2, just as expected from (27).

E. *Impedance chart*

Equivalent circuit approach opens new insights to RFID tag analysis and design. For example, we can better understand RFID tag performance by creating a new antenna impedance chart in natural circuit coordinates as explained below.

Recall that RFID chip impedance can be represented as a parallel circuit combination of R_p and C_p. This representation holds well across a wide range of frequencies where chip parallel resistance and capacitance remain constant. Hence, R_p and C_p are natural coordinates for the chip impedance. In these coordinates, at any specific power level (such as threshold power) chip impedance is just a single fixed point at all frequencies. This makes it different from Smith chart or Kurokawa chart (Smith chart modified for complex source impedances [48]), where analyzing an RFID tag (where series chip and antenna impedances are both complex and strongly frequency dependent) requires a frequency-dependent normalization.

What if we now plot our frequency-dependent antenna impedance in those new coordinates? The antenna impedance of the tag in our example is inductive at all frequencies of interest. Let us take a complex conjugate of it (that would make it capacitive) and then convert to parallel impedance form (find equivalent parallel resistance and capacitance). Then we can normalize those to chip R_p and C_p and plot using the same axis.

The plot shown in Fig. 18 shows the trajectories of our tag antenna impedance in air and on dielectric as functions of frequency. The horizontal axis is parallel resistance (normalized to chip R_p) and the vertical axis is parallel capacitance (normalized to chip C_p). Lower and higher POTF resonance frequencies are marked on each antenna curve: for air (ω_a =890 MHz, ω_a =1060 MHz) and for dielectric (ω_a =810 MHz, ω_a =935 MHz).

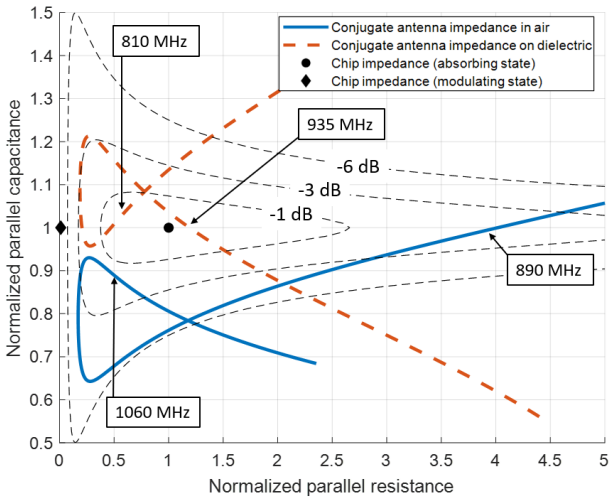

Fig. 18. Rp-Cp plot.

The axes in Fig. 18 are normalized to parallel chip impedance (R_p and C_p). For any tag that is made of specific antenna and a specific chip, antenna impedance can be easily plotted in those coordinates. Point (1,1) in Fig. 18 always represents the chip impedance in absorbing state at threshold. The closer the antenna trajectory lies to the point (1,1), the better is the complex conjugate impedance match between the chip and the antenna. Point close to point (0,1) represents chip impedance in modulating state. One can see that antenna impedance trajectories of this tag show a compromise in impedance matching because this tag was designed for various items as required by ARC specs. Contours of constant mismatch in these coordinates are slightly frequency-dependent and have triangular shape. Fig. 18 includes the contours of -1 dB, -3 dB, and -6 dB impedance mismatch.

V. Conclusions

In this paper, we described an equivalent circuit model-based approach to analysis and design of one of the most common UHF RFID tag antenna structures, a T-matched dipole. This is a very common tag antenna type used in industry for flexible labels applied to various items.

We presented a derivation of analytical closed-form solutions for T-matched tag resonant frequencies as functions of tag equivalent circuit parameters. In those derivations, we used definitions that are common in RFID industry. We also demonstrated how to use an equivalent circuit model to analyze a practical RFID tag, 70x14 mm retail tag with M700 IC, on air and on dielectric. EM simulations of this tag POTF and POTR agree very well with measured data. We analyzed this tag using an extracted equivalent circuit and showed how the tag antenna can be further optimized by exploring the influence of circuit parameters on tag performance. We also introduced a new impedance chart for analyzing tag antenna impedance in natural chip coordinates system, where chip impedance is a fixed point.

Proper tag design is very important for good overall RFID system performance. Any tag can be analyzed, understood, and optimized using an equivalent circuit approach, and the formulas derived in this paper further provide an additional insight for engineers and researchers. For example, the equivalent circuit and impedance chart described in this paper can be used to model and understand many RFID tag effects such effect of contact resistance, parasitic capacitance, strap capacitance (all of those can easily be added to the equivalent circuit), effect of capacitors in self-tuning RFID ICs [49, 50], effect of modulator impedance, etc.

We hope that this paper will be useful to a wide audience of tag antenna designers who want a deeper understanding of T-matched RFID tag antennas to design better tags for various applications.

References

[1] J. Landt, "The history of RFID," IEEE Potentials, vol. 24, no. 4, pp. 8-11, Oct.-Nov 2005.

[2] What is RAIN RFID Technology [Online]. Available : https://rainrfid.org/what-is-rain-rfid/

[3] A. Motroni, G. Cecchi, A. Ria and P. Nepa, "Passive UHF-RFID Technology: Integrated Communication, Localization and Sensing," in IEEE Journal of Radio Frequency Identification, vol. 7, pp. 564-572, 2023

[4] H. A. Wheeler, "Fundamental Limitations of Small Antennas," in Proceedings of the IRE, vol. 35, no. 12, pp. 1479-1484, Dec. 1947

[5] P. R. Foster and R. A. Burberry, "Antenna problems in RFID systems," IEE Colloquium on RFID Technology (Ref. No. 1999/123), London, UK, 1999, pp. 3/1-3/5

[6] K. V. S. Rao, P. V. Nikitin and S. Lam, "Antenna design for UHF RFID tags: a review and a practical application," IEEE Transactions on Antennas and Propagation, vol. 53, no. 12, pp. 3870-3876, Dec. 2005

[7] G. Marrocco, "Gain-optimized self-resonant meander line antennas for RFID applications," in IEEE Antennas and Wireless Propagation Letters, vol. 2, pp. 302-305, 2003

[8] R. Hansen, "Folded and T-matched dipole transformation ratio," IEEE Trans. on AP, vol. 30, no. 1, pp. 161-162, Jan. 1982

[9] Q. -X. Chu, L. Wang and J. -K. Zhou, "A Novel Folded T-matched Dipole in Base Station," 2007 International Conference on Microwave and Millimeter Wave Technology, Guilin, China, 2007, pp. 1-3

[10] Son H-W, Pyo C-S. "Design of RFID tag antennas using an inductively coupled feed", Electronics Letters, 2005, 41(18), pp. 994–992

[11] G. Marrocco, "The art of UHF RFID antenna design: impedance-matching and size-reduction techniques," in IEEE Antennas and Propagation Magazine, vol. 50, no. 1, pp. 66-79, Feb. 2008

[12] L. Ukkonen and L. Sydänheimo, "Impedance matching considerations for passive UHF RFID tags," 2009 Asia Pacific Microwave Conference, Singapore, 2009, pp. 2367-2370

[13] J. Choo, J. Ryoo, J. Hong, H. Jeon, C. Choi, and M. M. Tentzeris, "T-matching networks for the efficient matching of practical RFID tags," in 2009 European Microwave Conference (EuMC), Rome, Italy, Sep. 2009, pp. 5–8.

[14] D. D. Deavours, "Analysis and design of wideband passive UHF RFID tags using a circuit model," in 2009 IEEE International Conference on RFID, Orlando, FL, Apr. 2009, pp. 283–290

[15] N. A. Mohammed, K. R. Demarest and D. D. Deavours, "Analysis and synthesis of UHF RFID antennas using the embedded T-match," 2010 IEEE International Conference on RFID (IEEE RFID 2010), Orlando, FL, USA, 2010, pp. 230-236

[16] J. Xi and T. T. Ye, "Wideband and material-insensitive RFID tag antenna design utilizing double-tuning technique," 2011 IEEE International Symposium on Antennas and Propagation (APSURSI), Spokane, WA, USA, 2011, pp. 545-548

[17] E. Perret, S. Tedjini and R. S. Nair, "Design of Antennas for UHF RFID Tags," in Proceedings of the IEEE, vol. 100, no. 7, pp. 2330-2340, July 2012

[18] G. Zamora, S. Zuffanelli, F. Paredes, F. Martin, and J. Bonache, "Design and synthesis methodology for UHF-RFID tags based on the T-match network," IEEE Trans. MTT, pp. 4090-4098, Dec. 2013

[19] M. T. Reich and C. Bauer-Reich, "UHF RFID impedance matching: When is a T-match not a T-match?," 2014 IEEE International Conference on RFID (IEEE RFID), Orlando, FL, USA, 2014, pp. 23-30

[20] S. Shao, A. Kiourti, R. J. Burkholder and J. L. Volakis, "Broadband Textile-Based Passive UHF RFID Tag Antenna for Elastic Material," in IEEE Antennas and Wireless Propagation Letters, vol. 14, pp. 1385-1388, 2015

[21] F. Z. Gourari, S. M. Meriah, S. Protat, J. Dubouil and J. M. Laheurte, "Comparison of two matching techniques for UHF RFID tags," Microwave and Optical Technology Letters, vol. 60, p. 1763, 2018

[22] P. Nikitin, J. Kim, G. Berzagui, J. M. Roehe and K. Rao, "Reversed T-matching in RFID Tag Antennas," 2022 IEEE International Symposium on Antennas and Propagation and USNC-URSI Radio Science Meeting (AP-S/URSI), Denver, CO, USA, 2022, pp. 119-120

[23] Cho, C., Choo, H., Park, I.: 'Design of planar RFID tag antenna for metallic objects', Electron. Lett., 2008, 44, (3), pp. 175–177

[24] J. Choo and J. Ryoo, "UHF RFID Tag Applicable to Various Objects," in IEEE Transactions on Antennas and Propagation, vol. 62, no. 2, pp. 922-925, Feb. 2014

[25] F. Erman, S. Koziel and L. Leifsson, "Broadband/Dual-Band Metal-Mountable UHF RFID Tag Antennas: A Systematic Review, Taxonomy Analysis, Standards of Seamless RFID System Operation, Supporting IoT Implementations, Recommendations, and Future Directions," in IEEE Internet of Things Journal, vol. 10, no. 16, pp. 14780-14797, 15 Aug.15, 2023

[26] ARC Program [Online]. Available: https://rfid.auburn.edu/arc/

[27] T. G. Tang, Q. M. Tieng and M. W. Gunn, "Equivalent circuit of a dipole antenna using frequency-independent lumped elements," in IEEE Transactions on Antennas and Propagation, vol. 41, no. 1, pp. 100-103, Jan. 1993

[28] M. Hamid and R. Hamid, "Equivalent circuit of dipole antenna of arbitrary length," in IEEE Transactions on Antennas and Propagation, vol. 45, no. 11, pp. 1695-1696, Nov. 1997

[29] T. L. Simpson, "A Wideband Equivalent Circuit Electric Dipoles," in IEEE Transactions on Antennas and Propagation, vol. 68, no. 11, pp. 7636-7639, Nov. 2020

[30] P. Scholz, W. Ackermann, T. Weiland and C. Reinhold, "Antenna Modeling for Inductive RFID Applications Using the Partial Element Equivalent Circuit Method," in IEEE Transactions on Magnetics, vol. 46, no. 8, pp. 2967-2970, Aug. 2010

[31] A. P. Sample, D. T. Meyer and J. R. Smith, "Analysis, Experimental Results, and Range Adaptation of Magnetically Coupled Resonators for Wireless Power Transfer," in IEEE Transactions on Industrial Electronics, vol. 58, no. 2, pp. 544-554, Feb. 2011

[32] W. -Q. Niu, J. -X. Chu, W. Gu and A. -D. Shen, "Exact Analysis of Frequency Splitting Phenomena of Contactless Power Transfer Systems," in IEEE Transactions on Circuits and Systems I: Regular Papers, vol. 60, no. 6, pp. 1670-1677, June 2013

[33] P. Nikitin, J. Kim and K. Rao, "RFID Tag Analysis Using an Equivalent Circuit," 2021 IEEE International Symposium on Antennas and Propagation and USNC-URSI Radio Science Meeting (APS/URSI), Singapore, Singapore, 2021, pp. 167-168

[34] Voyantic - RFID and NFC Testing and Measurement Solutions [Online]. Available: https://voyantic.com

[35] J. D. Griffin and G. D. Durgin, "Complete Link Budgets for Backscatter-Radio and RFID Systems," IEEE Antennas and Propagation Magazine, vol. 51, no. 2, pp. 11-25, April 2009

[36] A. Lazaro, D. Girbau and D. Salinas, "Radio Link Budgets for UHF RFID on Multipath Environments," in IEEE Transactions on Antennas and Propagation, vol. 57, no. 4, pp. 1241-1251, April 2009

[37] P.V. Nikitin, K.V.S. Rao, R.D. Martinez, “, Differential RCS of RFID tag”, Electronics Letters, Volume 43, Issue 8, April 2007, p. 431 – 432

[38] N. Barbot, O. Rance and E. Perret, "Differential RCS of Modulated Tag," in IEEE Transactions on Antennas and Propagation, vol. 69, no. 9, pp. 6128-6133

[39] F. de Leon, A. Farazmand and P. Joseph, "Comparing the T and π Equivalent Circuits for the Calculation of Transformer Inrush Currents," in IEEE Transactions on Power Delivery, vol. 27, no. 4, pp. 2390-2398, Oct. 2012

[40] R. D. Middlebrook, "The two extra element theorem," Proceedings Frontiers in Education Twenty-First Annual Conference. Engineering Education in a New World Order, West Lafayette, IN, USA, 1991, pp. 702-708

[41] P. Nikitin, M. Brewster, J. Kim and K. Rao, "Dielectric Sensing using T-matched RAIN RFID Tags," 2023 IEEE International Conference on RFID (RFID), Seattle, WA, USA, 2023, pp. 42-47

[42] P. Nikitin, M. Brewster, J. Kim and K. Rao, "Magnetic Sensing using T-matched RAIN RFID Tags," 2024 IEEE International Conference on RFID (RFID), Boston, MA, 2024

[43] Impinj M700 series RAIN RFID tag chips [Online]. Available: https://www.impinj.com/products/tag-chips/impinj-m700-series

[44] P. Nikitin, J. Kim, and K. Rao, "RFID Tag Antenna Design for ARC Specs," 2020 IEEE International Symposium on Antennas and Propagation and USNC-URSI Radio Science Meeting (AP-S/URSI), Momtreal, Canada, 2020

[45] Beontag E702 RFID Wet Inlay (M750) [Online]. Available : https://www.atlasrfidstore.com/beontag-e702-rfid-wet-inlay-m750

[46] CST Studio Suite – Electromagnetic Field Simulation Software [Online]. Available: https://www.3ds.com/products/simulia/cst-studio-suite

[47] D. Caratelli, N. Haider and A. Yarovoy, "Analytically based extraction of Foster-like frequency-independent antenna equivalent circuits," 2013 International Symposium on Electromagnetic Theory, Hiroshima, Japan, 2013, pp. 506-509

[48] K. Kurokawa, "Power Waves and the Scattering Matrix," in IEEE Transactions on Microwave Theory and Techniques, vol. 13, no. 2, pp. 194-202, March 1965

[49] M. C. Caccami and G. Marrocco, "Electromagnetic Modeling of Self-Tuning RFID Sensor Antennas in Linear and Nonlinear Regimes," in IEEE Transactions on Antennas and Propagation, vol. 66, no. 6, pp. 2779-2787, June 2018

[50] K. Zannas, H. El Matbouly, Y. Duroc and S. Tedjini, "Self-Tuning RFID Tag: A New Approach for Temperature Sensing," in IEEE Transactions on Microwave Theory and Techniques, vol. 66, no. 12, pp. 5885-5893, Dec. 2018